



# Physically-based sound synthesis software for Computer-Aided-Design of piano soundboards

Benjamin Elie<sup>1,\*</sup>, Benjamin Cotté<sup>1</sup>, and Xavier Boutillon<sup>2</sup>

<sup>1</sup> IMSIA, UMR 9219 CNRS-EDF-CEA-ENSTA Paris, Institut Polytechnique de Paris, Chemin de la Hunière, 91120 Palaiseau, France

<sup>2</sup> Laboratoire de Mécanique des Solides, UMR 7649 École Polytechnique-Institut Polytechnique de Paris-CNRS, Rte de Saclay, 91120 Palaiseau, France

Received 24 November 2021, Accepted 22 June 2022

**Abstract** – The design of pianos is mainly based on empirical knowledge due to the lack of a simple tool that could predict sound changes induced by modifications of the geometry and/or the mechanical properties of the soundboard. We introduce the concept of Sound Computer-Aided Design through the framework of a program that is intended to simulate the acoustic results of virtual pianos. The calculation of the sound is split into four modules that compute respectively the modal basis of the stiffened soundboard, the string dynamics excited by the hammer, the soundboard dynamics excited by the string vibration, and the sound radiation. The exact resemblance between synthesis and natural sounds is not the primary purpose of the software. However, sound synthesis of real and modified pianos are used as reference tests to assess our main objective, namely to reflect faithfully structural modifications in the produced sound, and thus to make this tool helpful for both instrument makers and researchers of the musical acoustics community.

**Keywords:** Piano acoustics, Musical instrument making, Mean bridge mobility, Tone decay

## 1 Introduction

Designs of stringed musical instruments have been modified throughout history via empirical approaches used by manufacturers. In the case of the piano, we intend here to present a new technological object that would facilitate this empirical approach by designing and testing virtual pianos. Indeed, the traditional approach led to marginal improvements of existing schemes which cannot overcome the existing limitations of the instruments, such as *killer octaves* [1]<sup>1</sup> frequently encountered by piano manufacturers. Although manufacturers may usually apply fine local adjustments on the instruments to fix some of these issues, the problem of timbre homogeneity along the tessitura

remains difficult to solve with an empirical approach. This is mainly due to the fact that building complete instruments with new designs is tremendously costly in terms of time and effort. As a consequence, the current slow pace of the trial and error process needs to be enhanced significantly for new ideas of soundboard designs to emerge that could potentially overcome the aforementioned issues related to stringed instruments manufacturing.

In the case of the piano, which is the subject of this paper, many studies have been made in the past in order to fully comprehend all of the physical phenomena that are involved in the tone production. For instance, many authors have studied the vibro-acoustic behavior of the piano soundboard, either by experimental characterization [2–7], or by proposing simplified models [8–11] or finite element models [6, 12]. The string behavior, including the hammer-string interaction and the string-bridge coupling, has also been studied by several authors [12–18].

All of the aforementioned studies contributed to a better understanding of the piano functioning and several models are now available to simulate numerically the different mechanisms of the piano tone production chain, from the hammer activation to the radiated sound. By gathering some of these different numerical methods, this paper presents a framework of a program for the Sound Computer-Aided Design (SCAD) of piano soundboards and coupling

\*Corresponding author: [bnjmn.elie@gmail.com](mailto:bnjmn.elie@gmail.com)

<sup>1</sup> In this text, which is no longer available online, Fandrigh discusses a soundboard modification named “diaphragming”. He adds:

It is our opinion that this type of diaphragming makes the tenor-treble area of the soundboard too thin giving it too much flexibility (it lowers the mechanical impedance) and makes it difficult to obtain good sustain particularly through what we call the “killer octave.” That’s the area around the fifth to sixth octave where it is often impossible to get good sustain no matter what you do to the hammers. That’s because it isn’t a hammer problem, it’s a soundboard problem [1].

to the strings. This includes the location where each string is attached to the soundboard. It is solely based on physical models of the instrument in playing situation, and thus provide to piano makers a simple tool to predict the acoustic characteristics of a virtual piano, in regards to its specific geometry and to the mechanical properties of the soundboard and string materials. Although the physical models require many input parameters and some expertise to be run, a large effort has been undertaken to make the tool as simple as possible so that it can be used by any piano maker. This sound synthesis framework is specifically designed such that it facilitates the trial and error process of piano manufacturing. It can also be used to investigate the vibroacoustic behavior of piano soundboards, including the relationship between the mechanics of the soundboards and the resulting sounds in playing situation, which is paramount when designing instruments. The software is capable of producing the sound corresponding to a single note or a complete piece of music, at the price of a longer computation duration.

This open-source SCAD program is made available for any piano maker or academic researcher in the form of a software, called MAESSTRO,<sup>2</sup> which offers several functionalities to assist the piano maker in the design process. The software is open source and the source code of the software is freely available [19]. The different functionalities of the sound synthesis framework MAESSTRO are the following: (i) entering the geometry and the materials of the soundboard via a Graphical User Interface (GUI), (ii) feeding MAESSTRO with MIDI files to be synthesized, (iii) simulating numerically the physical phenomena involved in the production of piano tones, (iv) post-processing the software outputs, and (v) creating audio files of synthesized piano tones.

Figure 1 represents the global functioning of the software. It consists in a sequence of software operations that yields output synthesized piano tones from inputs specified by the users, including the geometry and the materials of the virtual soundboards, the string set parameters, and the tones to be played. The normalized data about the geometry and the materials of the virtual soundboard can be defined with the help of a specifically designed GUI. The modal basis of the virtual soundboard is computed with either a semi-analytical model [11], or a finite-element method [12]. Both models use a light fluid approximation. To synthesize specific tunes, the user may directly give a MIDI file from which MAESSTRO extracts the tone information, namely the note index, the key activation and release instants, as well as the hammer initial velocity. A nonlinear finite-element model of string dynamics [12] is then used to compute the bridge excitation force applied by the struck strings. Using the elements of the modal basis of the virtual soundboard, we can then compute the soundboard dynamics and the acoustic radiation at any listening point specified by the user.

This paper intends to demonstrate the possibilities of the software at characterizing the mechanical and acoustical behavior of the piano soundboards, and also to investigate

the impact of structural modifications of soundboards. It details the different functionalities of the various blocks in Section 2, including the physical models that are used to simulate the physical phenomena involved in the production of piano tones. The rest of the paper presents a case study that is intended to highlight the interest of the software for piano makers and/or researchers. It consists in analyzing the differences in terms of mechanical behavior and acoustic features of a soundboard to which we made structural modifications. The mechanical and acoustical variations are analyzed globally and also locally. Indeed, this analysis is also performed note by note in order to tackle the important question of the timbre homogeneity. The virtual soundboards used for the study are presented in Section 3. Section 4 presents the results in terms of mechanical properties while the acoustic results are presented in Section 5. In the last sections, we present examples of structural modifications that may be considered as naive. However, even if one admits that any maker is capable of predicting the sounding effect of such modifications, this prediction capability is itself the result of a rather long process of building plates, tables and sounding them in realistic conditions (excitation with strings under tension, for example): a lot of practical work. This tool simply shortens this process.

## 2 Functionalities of the MAESSTRO software

### 2.1 Using the software

Since the physical models of the MAESSTRO software may require long computations using large amounts of memory, we chose to propose to standard users to run their simulation on external servers that possess large memory capabilities. This solution also presents the advantage to remove the software installation process on the personal computer of each users, which may result in various OS compatibility issues. For standard users, the software is accessible in the numerical platform Simulagora,<sup>3</sup> developed by the company Logilab. The user will have to ask for opening an account,<sup>4</sup> which comes with free hours of simulations. Then, the user just has to upload the data online and to run the simulation. The data include the geometry of the virtual soundboard, the string set parameters, the note or the piece of music to be played (stored in the MIDI file), and a material dictionary containing the mechanical properties of the materials used to build the soundboard.

### 2.2 Computer-Aided-Design of the virtual soundboard

The software needs data about the geometry of the virtual soundboard and about the mechanical properties of its materials, which are gathered into a geometry file in a normalized format (JSON). In order to assist the user to build this geometry file, a specifically designed Graphical User Interface<sup>5</sup> has been developed in TypeScript with

<sup>3</sup> <https://www.simulagora.com/>.

<sup>4</sup> <https://www.maestro.cnr.fr/cao-sonore/>.

<sup>5</sup> It is available from any web browser at the following URL: <https://maestro.demo.logilab.fr/>.

<sup>2</sup> More information available at <https://www.maestro.cnr.fr>.

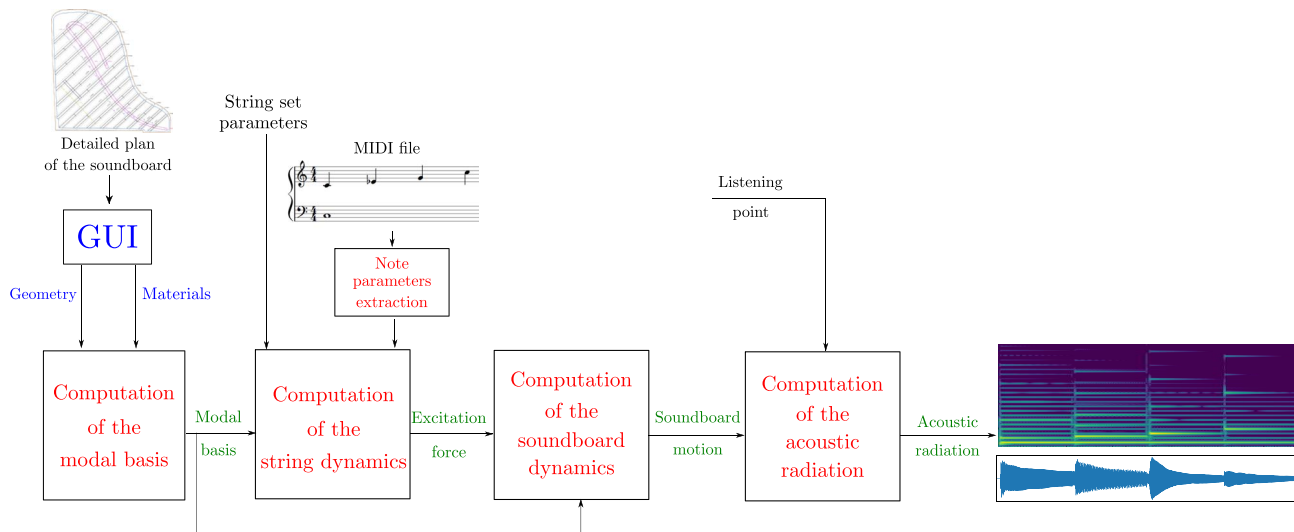


**Figure 1.** Block-diagram of the software architecture. The input data provided by the user are represented by a black font color. Blue corresponds to user data entered in the GUI. The software operations and the software outputs are represented by the red and green font colors, respectively.

React language with the help of Logilab. The choice of developing our own GUI has been motivated by the fact that adapting geometric data from standard three-dimensional CAD commercial software to our modeling would have added too much complexity, including naming convention of the soundboard components (panel, bridge, ribs, etc.) to extract the corresponding volumes.

The computation of the soundboard dynamics considers three main classes of structural components of the soundboard geometry, namely the main panel, the bridges and the ribs. The GUI defines the characteristics that are specific to each class: the coordinates of the points defining the panel contour, the variation of the width and the thickness of the bridge along its median line, etc. An example of the drawing of a panel contour is shown in Figure 2.

In order to make easier to link the material properties to each structural object, the GUI involves a material dictionary: a specific material, identified with a label, is assigned to each object. The mechanical properties of the materials are stored in a tabular format in a comma-separated value file (CSV). This material dictionary may be edited online, or locally, on the user machine. The mechanical properties include the mass density, the Young modulus in both directions of the soundboard plane, the shear modulus, the Poisson coefficient, and the constant modal loss factor of the material.

### 2.3 Computation of the modal basis

Currently, the software proposes two different methods to compute the modal basis of the soundboard: a semi-analytical method derived from Trevisan *et al.* [11], which requires strong simplifications of the soundboard geometry, and a finite-element method, derived from the models proposed by Chabassier *et al.* [12].

For this paper, we chose to use the finite-element method, associated with the library Montjoie.<sup>6</sup> The mesh is generated automatically by the software GMSH [20] according to the geometry file created in the graphical user interface. The method to compute the modal basis of the soundboard is based on a Reissner–Mindlin model of a clamped soundboard at its boundaries. This choice has been motivated by the fact that the superstructures, i.e. the ribs and the bridges, are modeled by the thickness variation of the soundboard, assuming they are centered with respect to the neutral fiber, hence the choice of a thick plate model over a thin plate model.

In order to obtain accurate eigenmodes, we use an iterative method to choose the characteristic length and the discretization order. They are chosen such that the obtained solution is sufficiently close to the exact solution of the problem while keeping a reasonable computation cost. For that purpose, we first choose the characteristic length  $l_c$  of the mesh elements so that it is smaller than a quarter of the smallest bending wavelength  $\lambda_{\min}$  in the desired frequency range. For a given maximal modal frequency  $F_{\max}$ :

$$\lambda_{\min} = \sqrt{\frac{2\pi}{F_{\max}}} \left[ \frac{D_3}{\rho_p h_p} \right]^{1/4}, \quad (1)$$

where  $\rho_p$  is the mass density of the soundboard material,  $h_p$  is the panel thickness, and  $D_3$  is the rigidity modulus in the direction perpendicular to the fibers (the least stiff direction). This yields  $l_c = \frac{\lambda_{\min}}{4}$ . Then, a convergence method is used to estimate the optimal discretization order: this consists in computing the modal frequency of a few test modes (typically  $L = 5$ ) in the high frequency domain, where the numerical dispersion is the highest,

<sup>6</sup> Available at <https://www.math.u-bordeaux.fr/~durufle/montjoie/>.

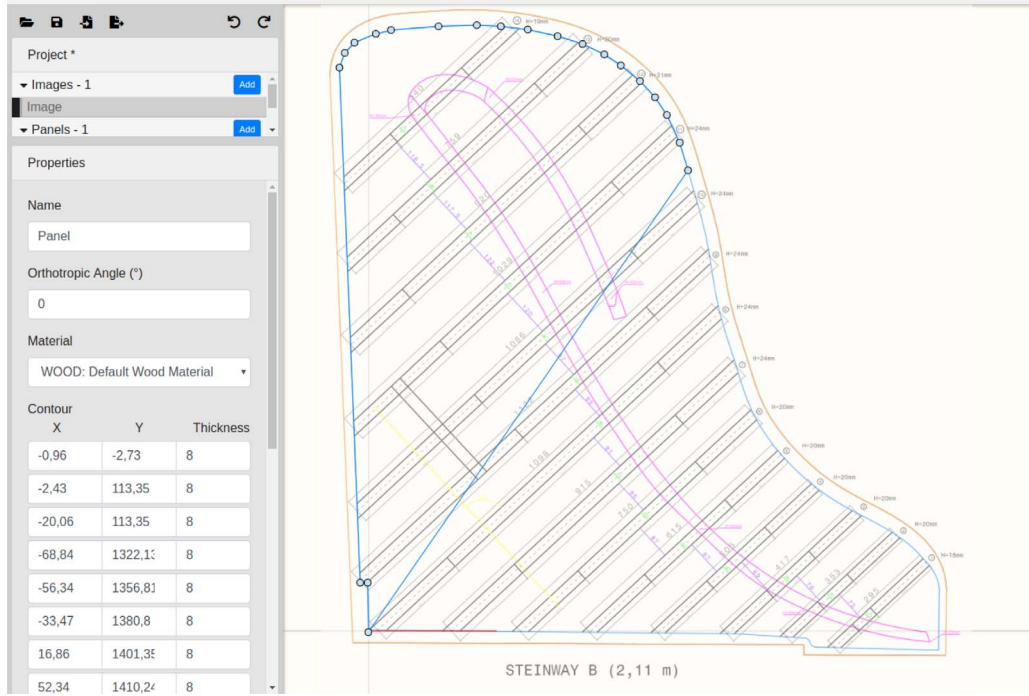


**Figure 2.** Screenshot of the MAESTRO GUI during the design of a panel contour.

for increasing orders. The chosen order  $k$  is taken as the smallest  $\tilde{k}$  that satisfies

$$k = \operatorname{argmin}_{\tilde{k} \in \mathbb{N}} \left( \frac{1}{L} \sum_{j=1}^L \left| \frac{f_j^{(\tilde{k}+1)} - f_j^{(\tilde{k})}}{f_j^{(\tilde{k})}} \right| < \epsilon \right), \quad (2)$$

where  $f_j^{(\tilde{k})}$  are the modal frequencies computed with order  $\tilde{k}$  and  $\epsilon$  is an arbitrary threshold. In the paper  $\epsilon = 10^{-6}$ , which leads to  $k = 3$  for all of the presented simulations.

The finite element computations are conservative. The modal shapes are real and we add an a posteriori modal loss factor to compute the bridge mobility. In our implementation, the user can only provide a constant modal loss factor using a material dictionary (see Sect. 2.2).

## 2.4 Simulation of the string dynamics

The dynamics of the string is simulated with a finite-element scheme derived from Chabassier *et al.* [12]. It considers a realistic hammer-string interaction model, a Timoshenko beam model for the string, and a *geometrically exact model* [21] to account for non linearity due to local geometric deformation of the string. We impose a null mobility condition at one end of the string and a soundboard transverse mobility at the other end, namely the string end attached to the bridge, as described in Figure 3. Following Chabassier *et al.* [12], the choice of the Timoshenko model is motivated by both physical and numerical reasons: its prediction is in good agreement with experimental data in a frequency range larger than the Euler-Bernoulli model.

The hammer model considers a memory model [22, 23] to compute the impact force of the hammer into the string

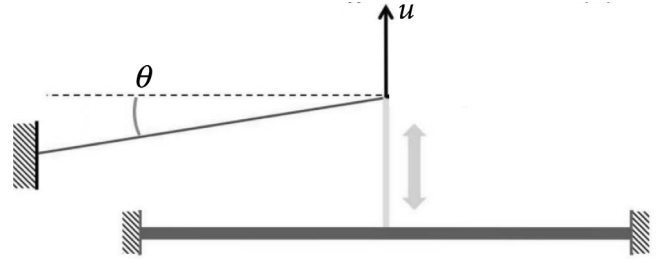


**Figure 3.** Figure and caption reproduced from Chabassier *et al.* [12]. Schematic view of strings-soundboard coupling at the bridge. The bridge is supposed to have a displacement  $u$  only along the vertical direction. The string forms a small angle  $\theta$  with the horizontal plane.

as a function of the felt deformation and of its viscoelastic properties. Since some parameters related to inner string damping or related to the hammer properties are very difficult to measure in real life experiments, especially for piano makers, we consider default values. They are taken from Chabassier and Duruflé [24], in which the authors propose the following empirical laws to estimate the hammer properties and the intrinsic damping coefficient of the strings:

$$\begin{cases} R_{u,i} = R_{\phi,i} = \alpha i + \beta \\ R_{v,i} = 0.5 \\ \eta_{u,i} = \eta_{\phi,i} = \gamma i + \delta \\ \eta_{v,i} = 10^{-9} \end{cases}, \quad (3)$$

where  $\alpha = 5 \times 10^{-3} \text{ s}^{-1}$ ,  $\beta = -0.015 \text{ s}^{-1}$ ,  $\gamma = 2.78 \times 10^{-11} \text{ s}$ , and  $\delta = 1.5274 \times 10^{-9} \text{ s}$ .  $R$  and  $\eta$  are respectively the fluid damping coefficient, in  $\text{s}^{-1}$ , and the viscous

damping coefficient, in  $s^{-1}$ , and indices  $\cdot_u$ ,  $\cdot_v$  and  $\cdot_\phi$  denote the transverse vibration, the longitudinal vibration, and the shearing, respectively.

Our model also accounts for multiple stringing. Consequently, the number of strings per note should be specified in input. Note that for the sake of simplicity, every string in the multiple stringing share the same parameters, including the coupling point with the bridge. Yet, it is possible to fine tune each string by multiplying the fundamental frequency of the note by a detuning factor.

Note that the longitudinal component of the string vibration is taken into account by choosing an angle  $\alpha$  between the string direction and the soundboard normal which is different from 90 degrees exactly [12]. The longitudinal vibration of the string comes from the nonlinear model of the string, due to its geometrically exact character, and from the excitation of the hammer. Longitudinal and transverse vibrations are coupled by the angle  $\theta$ , as shown in Figure 3, taken from [12]. The choice of the angle  $\theta$  can be modified by the user.

## 2.5 Computation of the soundboard dynamics

Once the displacement of the string is simulated, the transverse force applied to the bridge can be computed, as well as the resulting soundboard dynamics. The motion  $u_i$  of the table at time  $t$  in response to the transverse force applied by the string  $i$  is given by

$$u_i(x, y, t) = \sum_{j=1}^{N_{\text{modes}}} q_i^j(t) \Phi^j(x, y), \quad (4)$$

where  $q_i^j(t)$  is the modal coordinate at time  $t$  associated to the  $j$ th mode, and  $\Phi^j(x, y)$  is its mode shape.

## 2.6 Computation of the sound radiation

Finally, considering a point  $M$  in a three dimensional pressure field around the soundboard, defined by its coordinates  $\{x, y, z\}$ , the radiated sound pressure  $p(M, t)$  is computed using the Rayleigh integral assuming the soundboard is inserted in an infinite baffle (at  $z = 0$ ). Thus, for  $z > 0$ :

$$p(x, y, z, t) = \frac{j\rho_a c k}{2\pi} \int_S \dot{u}_s(x_s, y_s, t) \frac{e^{-jkd}}{d} dx_s dy_s, \quad (5)$$

where  $\rho_a$  is the air mass density,  $c$  is the sound speed,  $S$  is the surface area of the soundboard, and  $d = \sqrt{(x - x_s)^2 + (y - y_s)^2 + z^2}$  is the distance from the source point to the listening point  $M$ .

## 2.7 Numerical efficiency

The parameters for the numeric schemes are chosen so that the trade-off between fast computation and accuracy is optimized. For the simulations, we used the memory optimized computer available on Simulagora, which is a UNIX machine with 4 CPU processors at 2.3 GHz. The computation time for the modal basis, up to 5 kHz, using

a third-order finite element model is about 2 h. For the string dynamics, the computation depends strongly on the simulated note. Indeed, due to the presence of harmonic of higher orders in the frequency range of interest, bass strings require a larger number of spatial discretization points than treble strings, which slows down the simulations. The value of the simulation frequency is related to the nonlinear model of string that is used. It is set so that we obtain a good precision of the string eigenfrequencies. With the nonlinear model used for the string dynamics, a simulation frequency of 10 MHz has been found to provide a good accuracy. The simulation of the central C3 during 2 s takes 16 min and 30 s. We are currently planning to optimize the codes, with parallel programming, for instance. Finally, the computation of the acoustic radiations takes 31 s. Note that for the acoustic radiation, it is not necessary to set a simulation frequency as high as for the string dynamics. As a consequence, the simulation frequency, which is the sampling frequency of the output audio file, is set to  $2.1F_{\text{max}}$ , where  $F_{\text{max}}$  is the maximal modal frequency. Note that the semi-analytical method to compute the modal basis (see Trevisan *et al.* [11]) is much faster (it takes around 700 s to compute the modal basis up to 5000 Hz) at the cost of the loss of fine geometric details [25].

## 3 Applications: virtual soundboards

The models used in the software have all been previously published, where they have been compared to experimental data. The reader may find such comparisons in the original papers. For instance, in [11], the mode shapes obtained using the semi-analytical model by Trevisan *et al.* have been compared with those obtained experimentally on an upright piano (Pleyel P131), and have been shown to be in good agreement. Chabassier *et al.* [12] compared the simulation of the string motion of a virtual and a real Steinway D. The simulated string motion exhibits the same inharmonicity profile as the measured string of the Steinway D. Additionnally, the model has also been proven in [12] to be able to accurately simulate phenomena observed in real pianos, such as the dependance of frequency with amplitude, the presence of soundboard modes in the initial transient of the tones, and the presence of phantom partials.

The main objective of the software is to be able to reproduce sound variations due to structural modifications. Therefore, as an illustration of the different functionalities of the MAESSTRO software, we present in this paper a preliminary study that compares the mechanical and acoustical properties of different virtual soundboards only. The virtual soundboards consist in a reference piano, derived from a real piano, which is subject to several modifications to evaluate their mechanical and acoustical impacts. The chosen modifications include the increase of the panel thickness, the removal of half the ribs, and the removal of all the ribs. This results in four cases, namely the reference piano (RP) and the three modified pianos (MP1, MP2, and MP3). These modifications correspond

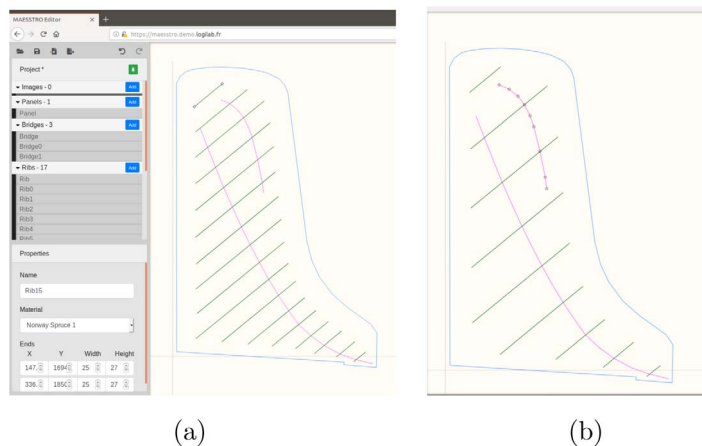


**Figure 4.** Screen shot of the GUI after completion of the design of the virtual Steinway D. The panel contour is shown in blue, the median line of the bridges in pink and the median lines of the ribs in green. Left (a) is the reference piano, right (b) is the modified piano 2, labeled as MP2

to change in stiffness, namely a global increase for MP1, a local decrease for MP2, and both a global and local stiffness decreases for MP3. Although this is unlikely to be representative of what piano manufacturer would try in real life, we chose these caricatural structural modifications of the reference piano in order to emphasize their mechanical and acoustical impacts in the resulting tones. Besides, these gross modifications make the qualitative prediction of the variations in the mechanical behavior and some acoustic features possible.

### 3.1 Reference piano

The reference piano geometry is a simplified version of the Steinway D. The geometric data has been extracted via the MAESTRO GUI, as shown in Figure 4. We chose to simplify the geometry of the Steinway D in order to present a study on a generic piano with realistic dimensions and properties instead of a particular piano. Simplifications include a constant panel thickness over the whole surface, constant bridge height, and the removal of the tapered section of each ribs. The dimensions of the different elements of the soundboard are detailed in Table 1, and the mechanical properties of the materials in Table 2. The resulting mesh contains 23,006 elements.

### 3.2 Modified pianos

The first modified piano (labeled as MP1) is similar to the reference piano RP except that the thickness of the soundboard is twice the one of RP, namely 16 mm. The second modified piano, MP2, is similar to RP but with inter-rib spacing twice as RP (see Fig. 4b). Finally, the third modified piano, MP3, is similar to RP but without ribs: all ribs have been removed and the bridges are the only superstructures.

Strings are assumed to be the same from a virtual soundboard to the next. The parameters of the string set are taken from a technical report [24], which provides all

of the required information to compute the dynamics of any string of the virtual reference piano, including string geometry and tension, Young modulus of the string materials, internal damping, and location of the bridge coupling points. It also provides the mechanical parameters of the hammers, namely the mass, the stiffness, and the impact location on the string, as detailed in Section 2.4. For this study, we used the wrapped strings model of [24]. We chose these values because they have been defined for a Steinway D simulation.

## 4 Effect of structural modifications on mechanical quantities

This section discusses the differences in mechanical behavior between the virtual soundboards. The impact of stiffness variations of plate-like structures on some mechanical parameters, such as the modal density and the mobility, is well-known, and this section aims at verifying that the stiffness modifications compared to RP cause the expected effects to the mechanical parameters.

### 4.1 Modal density

The modal density, denoted  $n(f)$ , is a measure of the number of modes in a frequency band. In this paper, we define the modal density as the inverse of the frequency spacing between two successive modes, hence

$$n(f_k) = \frac{1}{f_{k+1} - f_k}, \quad (6)$$

where  $f_k$  is the modal frequency of the  $k$ th mode, and  $f_k = \frac{1}{2}(f_{k+1} + f_k)$ . In practice, since the modal spacing may vary significantly, we apply a moving average for six successive modes to smooth the modal density curve.

For plate-like structure, the modal density is known to tend asymptotically at high frequencies toward a

**Table 1.** Geometric data of the elements of the reference piano.

Quantity	Unit	Object			
		Panel	Bridge #1 (bass)	Bridge #2 (treble)	Ribs
Angle of fiber orientation	degree	135	–	–	–
Thickness	mm	8	60	20	17 (treble rib) to 27 (bass rib)
Width	mm	–	32	32	21 (treble rib) to 25 (bass rib)
Material		Sitka spruce	Beech	Beech	Sitka spruce

**Table 2.** Mechanical properties of the materials used for the study.  $\rho$  is the mass density,  $E_x$  and  $E_y$  are the Young modulus in the  $x$  and  $y$  direction, respectively.  $G$  denotes the shear modulus,  $\nu$  is the Poisson coefficient, and  $\eta$  is the modal loss factor.

Material	$\rho$ (kg m <sup>-3</sup> )	$E_x$ (GPa)	$E_y$ (GPa)	$G_{xy}$ (GPa)	$G_{xz}$ (GPa)	$G_{yz}$ (GPa)	$\nu_{xy}$	$\eta$ (%)
Sitka spruce	380	11	0.650	0.66	1.2	0.042	0.26	2
Beech	750	13.7	2.24	1.61	1.06	0.46	0.3	2

constant, which has been estimated by Courant and Hilbert [26]:

$$n_\infty = \frac{S}{2} \sqrt{\frac{\rho h}{D}}, \quad (7)$$

where  $S$  is the surface of the plate and  $D$  is the bending stiffness. For isotropic materials,  $D = \frac{Eh^3}{12(1-\nu^2)}$ . For orthotropic materials, such as those used for piano soundboards, the expression of  $D$  is more complicated (see [27] for details) but still implies an increase with  $h^3$ . Given that relation between the bending stiffness and the plate thickness, the asymptotic modal density is proportional to  $h^{-1}$ . Additionally, it implies that stiffer plates have lower modal density as well as thicker plates. The behavior of the modal density in the low and the mid frequency domains depends on the boundary conditions. According to Xie *et al.* [28], the modal density of a clamped plate writes:

$$n(f) = n_\infty - \frac{1}{\sqrt{8\pi}} \left( \frac{\rho h}{D} \right) P f^{-1/2}, \quad (8)$$

where  $P$  is a geometric factor. Equation (8) shows an increasing modal density as a function of the frequency, which implies that the modal density of clamped plates tends towards the asymptotic value from lower values. These equations are used to understand the behavior of the modal density for our virtual soundboards. Indeed, we expect the following modal density tendencies: MP1 should have the lowest modal density and MP3 the highest. Between both soundboards, RP should have a lower modal density than MP1. Finally all should have growing modal density as a function of the frequency. These remarks are confirmed by Figure 5, which shows the modal density for the four soundboards as a function of the frequency. The modal density of the reference piano is qualitatively similar with that of an upright piano measured in [5], but with larger values. Given the smaller surface of upright soundboards in comparison to the

chosen reference piano, this is in agreement with our expectations.

## 4.2 Bridge mobility

The driving-point mechanical admittance (or mobility) quantifies the ability of a structure to vibrate under an excitation force. It is defined as the response, in velocity, of a structure to a unit force in the frequency domain, hence

$$Y_A(\omega) = \frac{V_A(\omega)}{F_A(\omega)}, \quad (9)$$

where  $V_A$  is the velocity and  $F_A$  the force applied to the structure at point  $A$ .

It can generally be developed on the basis of complex modes [29], but we assume the mode shapes are real. In such conditions, the mobility can be written as

$$Y_A(\omega) = j\omega \sum_{n=1}^N \frac{\Phi_n^2(x_A, y_A)}{m_n(\omega_n^2 + j\eta_n\omega_n\omega - \omega^2)}, \quad (10)$$

where  $\omega_n$ ,  $\eta_n$ ,  $m_n$  and  $\Phi_n$  are respectively the modal angular frequency, the modal loss factor, the modal mass and the modal shape associated to the  $n$ th mode.

The mobility is an essential feature that characterizes the mechanical behavior of dynamic structures. It has been widely studied in the case of stringed musical instruments as a characteristic parameter [3, 7, 10, 14, 30, 31]. Usually, the mobility is considered at the bridge-string coupling points, hence the so-called *bridge mobility*.

Recently, some researches in musical acoustics have focused on a synthetic description of the mobility via macroparameters [32, 33]. In these studies, the mean mobility has been proposed as an efficient parameter to characterize the global behavior of stringed instruments. Its definition is derived from the Skudrzyk's *mean-value theorem* [34], which introduces the characteristic admittance of a structure as the mobility of the equivalent structure with infinite dimensions. For plate-like structures, the characteristic admittance  $Y_C$  is

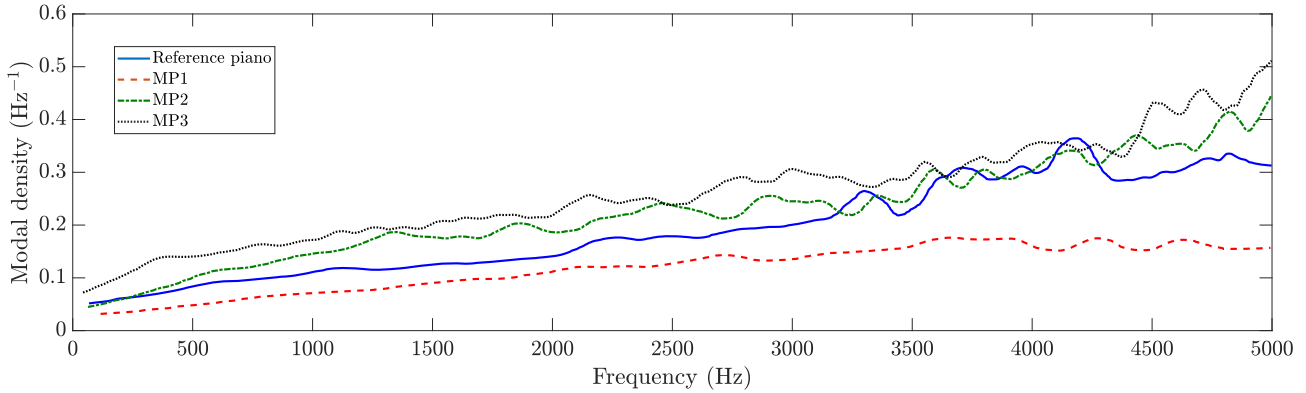


**Figure 5.** Modal density of the virtual soundboards as a function of the modal frequency.

$$Y_C = \frac{1}{8\sqrt{\rho h D}}. \quad (11)$$

As for the modal density, an increase of the global stiffness of the structure tends to lower the characteristic admittance. Additionally, the superstructures locally increase the stiffness of the soundboard, which may lead to local changes of the characteristic admittance: it is then a spatially-dependent quantity.

In practice, the characteristic admittance  $Y_C$  may be approached by taking the average value of the mobility over a sufficiently large frequency span [27]. For this study, we compute the bridge mobility for each of the string attachment points at the bridge, and then compute the average value of mobility. Following Skudrzyk's theorem, we choose to use the geometric mean of the mobility. The frequency range used to compute the mean mobility is 25–5000 Hz, hence

$$\langle Y_A \rangle = \left( \prod_{f=25\text{Hz}}^{f=5000\text{Hz}} |Y_A(f)| \right)^{1/N}, \quad (12)$$

where  $N$  is the number of frequency bins used to compute the bridge mobility  $Y_A$  at point  $A$  between 25 and 5000 Hz. Since the superstructures modify locally the characteristic admittance, the modifications of the rib pattern, as for MP2 and MP3, should be visible in the distribution of the mean mobility values along the bridge.

The computed mean mobility values along the bridge are displayed in Figure 6. The obtained values for the reference piano are of the same order of magnitude than values found in previous studies. For instance, Giordano provides in [4] an impedance curve, measured in the C4 position (note index 40) of an upright piano, with a mean value of about 1500 kg/s, which corresponds to a mean mobility of  $-63.5$  dB. In this range, the mean mobility of the reference piano is between  $-65$  and  $-63$  dB. Similar mobility values for upright and grand pianos are not surprising. Indeed, they are made with similar thickness and materials, and the characteristic admittance does not depend on the plate area by definition (Eq. (11) implies only the mass

density, the thickness and the stiffness of the plate). Consequently grand piano should present mobility values in the same order of magnitude as upright pianos.

Our simulations confirm that piano MP3, which is the least stiff, has the largest mean mobility and that MP1, which is the stiffest, has the lowest. Interestingly, the local variations of the mean mobility value due to the presence of the superstructures are clearly visible. For instance, since the bass bridge is higher than the other bridge in order to allow bass strings to fold over the medium strings (*cf.* Tab. 1), the soundboard is locally stiffer at the bass bridge. As a consequence, the mean mobility is much lower for the bass strings coupling points, corresponding to the note index 1–18, than the medium and treble strings. The gap is about 10 dB for 8 mm-thick soundboards (RP, MP2, and MP3), and about 5 dB for the 16 mm-thick soundboard (MP1). Additionally, the mean bridge mobility oscillates for soundboards that contain ribs: when a string is located on a rib, the mobility is lower whereas it is higher when the string is located far from a rib. It can be clearly seen for MP2, which has a large inter-rib spacing, where the mobility value reaches that of MP3 when the string is located far from a rib. For MP3, which has no ribs, the mobility value is almost constant in the medium and treble string range. It is interesting to note that the inter-rib spacing of the reference piano is such that it moderates the amplitude of the mean bridge mobility oscillation. In the high-medium string range (index 40–60), it is almost as homogeneous as MP3, whereas the mean bridge mobility of MP2 still oscillates with an amplitude of about 6 dB.

## 5 Effect of structural modifications on acoustic features

The previous section has shown that the impact of structural modifications of the piano soundboards could be visible in the mechanical properties, namely in the modal density and the average mobility along the bridge. It is now interesting to analyze the sound produced by the virtual soundboards to check if the structural modifications are



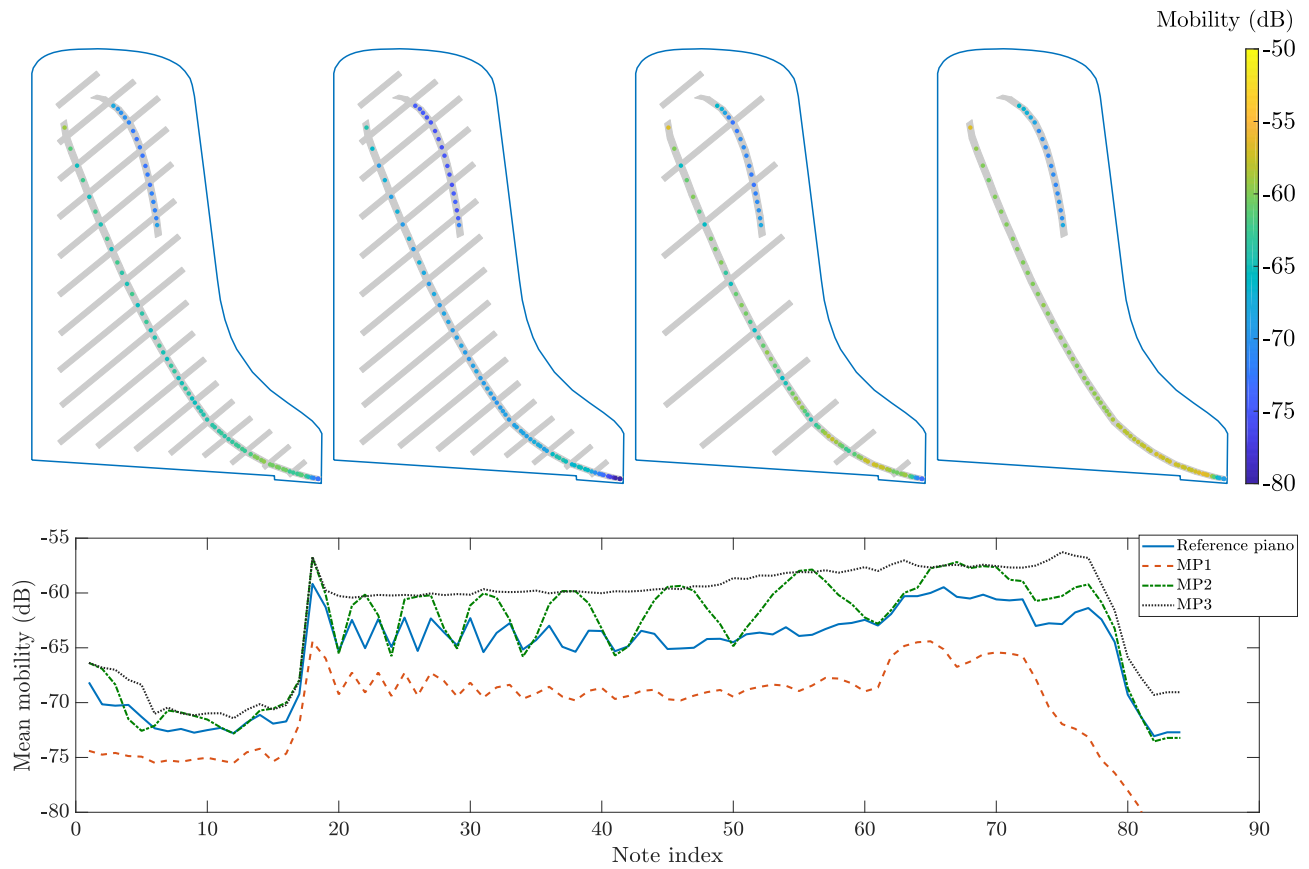


**Figure 6.** Mean mobility of the soundboard at the string-bridge coupling points. From left to right are the reference piano, the modified piano #1, the modified piano #2, and the modified piano #3. Bottom is the mean mobility as a function of the note index for the 4 virtual pianos.

also audible. This section presents acoustic features of the notes synthesized from the four virtual soundboards. The reader can listen to audio examples of a same note synthesized from the four studied virtual soundboards in the repository of the project (see the section [Data Availability Statement](#)). For the simulations, we considered the following strings-per-note distribution: notes 1–27 contain only one string, 2 strings for notes 28–51, and 3 strings for notes 52–88.

### 5.1 Acoustic features

Unlike the mechanical properties, the effect of the soundboard stiffness on the acoustic features of the piano sounds in playing situation is not fully understood. However, we assume the following hypotheses to be true:

*Hypothesis 1:* A soundboard with a high mobility level will be more responsive than a soundboard with a low mobility level, which will result in a more powerful acoustic response at its maximal energy level.

*Hypothesis 2:* A soundboard with a high mobility level will produce a sound with a faster decay. Indeed, the damping coefficient of the string due to the coupling with the mobile bridge is directly proportional to the level of the bridge mobility [14].

Considering these assumptions, this section analyzes the synthesized tones via two acoustic features, which are the maximal sound pressure level and the energy decay time.

The energy decay time is analyzed via the computation of the *Energy Decay Curves* (or EDC), introduced by Schroeder [35, 36]. It is defined as the amount of energy remaining in the signal at each time instant, hence

$$\text{EDC}(t) = \int_t^{\infty} p^2(\tau) d\tau. \quad (13)$$

Following room acoustics based methods, we define the decay time  $T_{15}$  as the time for which the first linear part of the EDC, expressed in dB, decreases by 15 dB. [Figure 7](#) shows an example of energy decay curve for a simulated A4 of the reference piano.

### 5.2 Results along the tessitura

For each virtual soundboard, the maximal sound pressure level and the decay time  $T_{15}$  have been computed for notes from C1 to G#7. [Figure 8](#) shows the evolution of the acoustic features along the tessitura for the four virtual soundboards. The raw values present large variations from a note to the next, especially for the decay time. In order to extract global trends, we also present the locally averaged

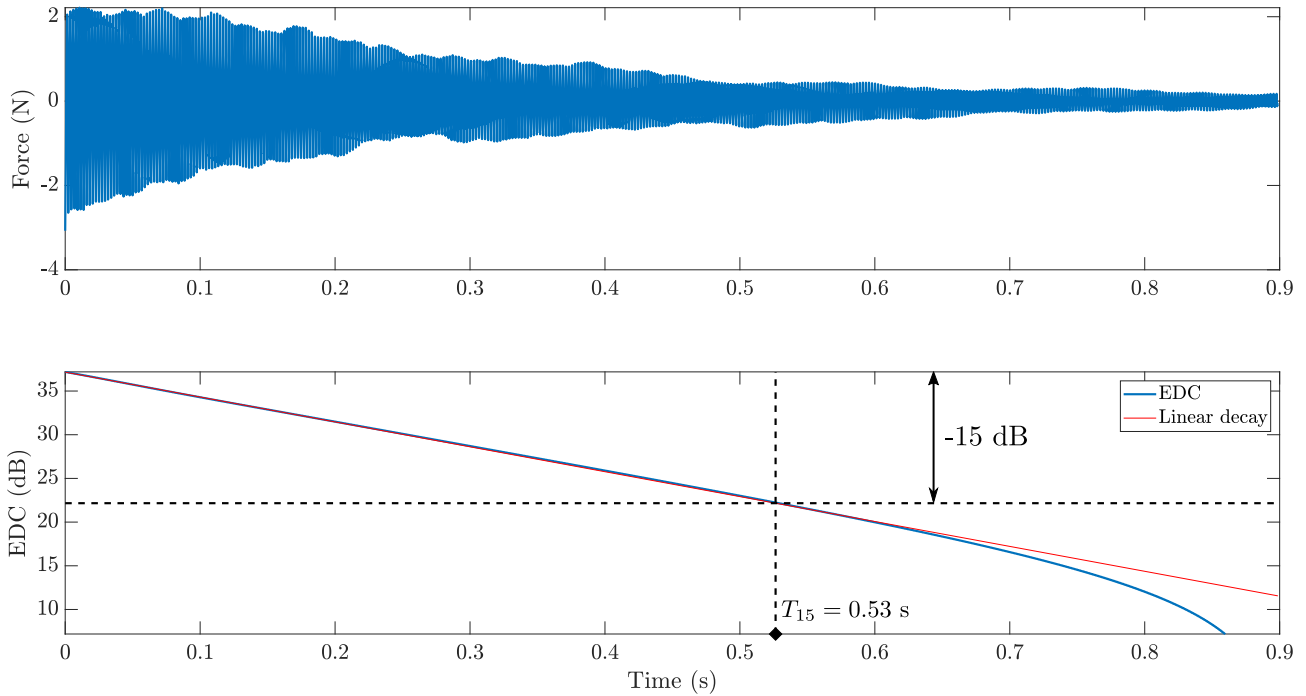


**Figure 7.** Example of energy decay curve (bottom) computed from the force applied by the A4 string to the soundboard of the reference piano (top). The linear part of the EDC (red solid line), obtained by linear interpolation, is used to compute the decay time  $T_{15}$ .

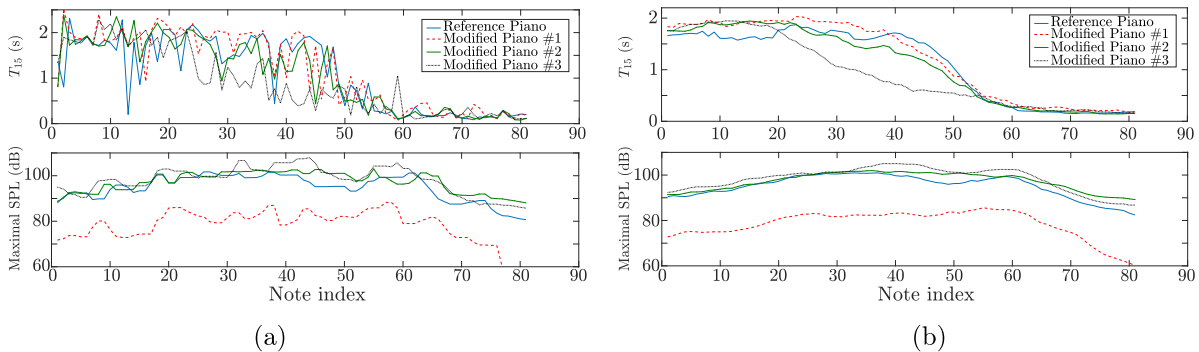


**Figure 8.** Energy decay time  $T_{15}$  (top) and maximal sound pressure level (bottom) computed from the simulated piano tones over the tessitura. Left (a) are the non-averaged features, and right (b) are the locally averaged features over an octave.

values, obtained from the mean value of a sliding window with a length of 12 notes (an octave). These values highlight some interesting points.

Firstly, the locally averaged maximal sound pressure levels confirm (Hyp. 1) expressed in Section 5.1, claiming that the maximal sound pressure level may be positively correlated to the mean mobility value: notes synthesized from MP1 present very low sound pressure levels in comparison with other soundboards, and notes from MP3 present the highest sound pressure levels. Additionally, the sound pressure levels in the bass and treble ranges are lower than in the medium range, following the same trend as the mean mobility.

Then, there is no significant differences in  $T_{15}$  between virtual soundboards, except for MP3, which, as expected,

presents much lower decay times. For the other soundboards, the mean value of mobility does not seem to have a significant influence on the decay time. Since the damping coefficient due to the coupling with the bridge is proportional to the mobility value at the string modal frequencies, this may change significantly between two notes, or between two similar notes but from different soundboards. This explains the large variations of the raw decay times and the fact that the rib pattern is not retrieved in the decay times. For MP3, one possible explanation of the lower decay time is the fact that the mobility level is such that the damping coefficient due to the coupling is more likely to be always of the same order of magnitude than the intrinsic string damping, and consequently to enhance the energy decay.

These results highlight the trade-off which is often mentioned by plucked and struck string instrument makers. When designing their soundboard, they have to make an instrument with a sufficiently high mobility to easily produce powerful sound, but not too high to ensure a reasonable sustain. In this example, although producing tones at higher sound pressure level than the reference piano by a few decibels, the energy decay of tones produced by MP3 is such that it is likely to be considered as a poor quality instrument.

## 6 Conclusions and future works

This paper has presented the framework for the Sound Computer-Aided Design of piano soundboards that is intended to help piano makers in the design process by giving them a tool to synthesize tones or short musical passages produced by virtual pianos. Case studies show the interest of the software in predicting mechanical and acoustical impacts of structural modifications of a piano soundboard. Indeed, starting from a reference piano, we defined three modified virtual pianos. Modifications have been chosen to reflect global or local variations of the stiffness. The impact of these stiffness variations on the soundboard mechanical behavior is in agreement with the theory of plate-like structures: lowering the soundboard stiffness increases the modal density and the mean mobility. Our simulations show that the rib pattern causes a local modification of the mean bridge mobility, which exhibits variations whether the string is attached near a rib or in the inter-rib area. Interestingly, the variation amplitude of mean bridge mobility is smaller for the reference piano than for a piano with an inter-rib spacing that is twice as that of the reference piano. This suggests that the inter-rib spacing of traditional pianos would have been empirically defined so that it makes the bridge mobility almost homogeneous along the bridge.

The impact of the global stiffness is also audible in the resulting sound pressure level: stiffer soundboards tend to produce less powerful tones. However, the local stiffness variations due to the variation of rib patterns are less visible. The chosen acoustic features for this study, namely the maximal sound pressure level and the decay time, exhibit large variations from note to note. One reason could be that the mobility curve pattern may have a more important influence on the acoustic features of one note than the mean mobility when comparing a few notes. However, when a large note scale is averaged, e.g. an octave, the acoustic features reflect the variations of the mean mobility. These observations also hold for the decay times, which show very large variations from note to note, but clear global tendencies can be observed from locally averaged values. Comparisons between virtual soundboards show that they all share similar decay times, except for the least stiff soundboard, which presents decay times much smaller in the medium range, from E2 to D5. This is probably due to the fact that, unlike other pianos, the mean mobility level is such that the damping coefficient due to the coupling with the bridge is sufficiently high to have a significant influence on the decay time.

If the piano makers adopt the software, they will be able to virtually test new designs, and thus significantly enhance the pace of the trial and error process. Thus, we are convinced that significant evolution of the traditional architecture of piano soundboards would emerge in the near future. The resulting synthesized piano sounds may however be still perceived as non-realistic, mainly because of the lack of fine and precise modeling of dissipative phenomena in both the soundboard and the strings. We emphasize here that the software ambition is to faithfully reflect variations. Of course, the absolute resemblance is valuable and its improvement will be addressed in the future. For instance, our simulations did not reproduce the double decay phenomenon, which has been observed in some piano tones [14], but certainly not in all of them. This limitation is due to the unique polarization of the string motion and of the sole consideration of the vertical motion of the bridge. Indeed, the coupling between the strings and the plate at the bridge relies on a very simple model in the software (continuity of the vertical velocity) but measurements on real pianos point towards a more complex model allowing rocking and horizontal motions of the bridge. One other major evolution could be the use of composite materials: the software could be used to predict the sound of a piano with soundboard made in specific composite materials, or even be used to find the mechanical properties which could yield to the sound desired by the piano maker. Finally, we also expect the software to be used by researchers, and thus become a useful tool of communication between piano makers and academic researchers. We are planning to modify the software with the help of academic partners to use it for other string instruments, such as the guitar.

## Acknowledgments

This work is part to the project MAESSTRO funded by French ANR (Agence Nationale de la Recherche). The authors would also like to thank Nicolas Chauvat, Denis Laxalde, Frank Bessou, and Viet-Hung Nhu from Logilab for the development and implementation of many modules of the software, including the Graphical User Interface.

## Data availability statement

The source code of the open-source software MAESSTRO [19] is freely available in the GitLab maestro repository (<https://gitlab.com/benjamin.elie/maestro>).

The maestro repository contains audio examples of synthesized piano tones (<https://gitlab.com/benjamin.elie/maestro/-/tree/master/examples/audio>).

Additional data are available on request from authors.

## References

1. D. Fandrich: Soundboard technology and manufacture. The Designer's Notebook, Piano Builders/NW, 1995.

2. H. Suzuki: Vibration and sound radiation of a piano soundboard. *Journal of the Acoustical Society of America* 80, 6 (1986) 1573–1582.
3. H.A. Conklin Jr: Design and tone in the mechanoacoustic piano. Part II. Piano structure. *Journal of the Acoustical Society of America* 100, 2 (1996) 695–708.
4. N. Giordano: Mechanical impedance of a piano soundboard. *Journal of the Acoustical Society of America* 103, 4 (1998) 2128–2133.
5. K. Ege, X. Boutillon, M. Rébillat: Vibroacoustics of the piano soundboard:(non) linearity and modal properties in the low- and mid-frequency ranges. *Journal of Sound and Vibration* 332, 5 (2013) 1288–1305.
6. A. Chaigne, B. Cotté, R. Viggiano: Dynamical properties of piano soundboards. *Journal of the Acoustical Society of America* 133, 4 (2013) 2456–2466.
7. R. Corradi, S. Miccoli, G. Squicciarini, P. Fazioli: Modal analysis of a grand piano soundboard at successive manufacturing stages. *Applied Acoustics* 125 (2017) 113–127.
8. N. Giordano: Simple model of a piano soundboard. *Journal of the Acoustical Society of America* 102, 2 (1997) 1159–1168.
9. J. Berthaut, M.N. Ichchou, L. Jézéquel: Piano soundboard: Structural behavior and numerical and experimental study in the modal range. *Applied Acoustics* 64 (2003) 1113–1136.
10. X. Boutillon, K. Ege: Vibroacoustics of the piano soundboard: Reduced models, mobility synthesis, and acoustical radiation regime. *Journal of Sound and Vibration* 332, 18 (2013) 4261–4279.
11. B. Trévisan, K. Ege, B. Laulagnet: A modal approach to piano soundboard vibroacoustic behavior. *Journal of the Acoustical Society of America* 141, 2 (2017) 690–709.
12. J. Chabassier, A. Chaigne, P. Joly: Modeling and simulation of a grand piano. *Journal of the Acoustical Society of America* 134, 1 (2013) 648–665.
13. H. Fletcher: Normal vibration frequencies of a stiff piano string. *Journal of the Acoustical Society of America* 36, 1 (1964) 203–209.
14. G. Weinreich: Coupled piano strings. *Journal of the Acoustical Society of America* 62, 6 (1977) 1474–1484.
15. X. Boutillon: Model for piano hammers: Experimental determination and digital simulation. *Journal of the Acoustical Society of America* 83, 2 (1988) 746–754.
16. A. Chaigne, A. Askenfelt: Numerical simulations of piano strings. I. A physical model for a struck string using finite difference methods. *Journal of the Acoustical Society of America* 95, 2 (1994) 1112–1118.
17. H.A. Conklin Jr: Design and tone in the mechanoacoustic piano. Part I. Piano hammers and tonal effects. *Journal of the Acoustical Society of America* 99, 6 (1996) 3286–3296.
18. H.A. Conklin Jr: Design and tone in the mechanoacoustic piano. Part III. Piano strings and scale design. *Journal of the Acoustical Society of America* 100, 3 (1996) 1286–1298.
19. B. Elie, B. Cotté, X. Boutillon, N. Chauvat, D. Laxalde, F. Bessou, V.-H. Nhu, B. Trévisan: MAESSTRO (version 1.0.0) [Code]. GitLab. 2021. <https://gitlab.com/benjamin.elie/maesstro>.
20. C. Geuzaine, J.-F. Remacle: Gmsh: A 3-D finite element mesh generator with built-in pre- and post-processing facilities. *International Journal for Numerical Methods in Engineering* 7911 (2009) 1309–1331.
21. P.M. Morse, K.U. Ingard: *Theoretical acoustics*. McGraw-Hill, New York. 1968.
22. A. Stulov: Hysteretic model of the grand piano hammer felt. *Journal of the Acoustical Society of America* 97, 4 (1995) 2577–2585.
23. A. Stulov: Experimental and theoretical studies of piano hammer, in *Proceedings of the Stockholm Music Acoustics Conference*, Vol. 485. 2003.
24. J. Chabassier, M. Duruffé: Physical parameters for piano modeling. Technical Report, INRIA, 2012 [Online]. Available <https://hal.inria.fr/hal-00688679v1/document>.
25. B. Elie, X. Boutillon, J. Chabassier, K. Ege, B. Laulagnet, B. Trévisan, B. Cotté, N. Chauvat: MAESSTRO: A sound synthesis framework for Computer-Aided Design of piano soundboards, in *ISMA 2019*, Detmold, Germany. 2019.
26. R. Courant, D. Hilbert: *Methods of Mathematical Physics*, Vol. 1, Wiley Classic Edition. 1989.
27. B. Elie, F. Gautier, B. David: Estimation of mechanical properties of panels based on modal density and mean mobility measurements. *Mechanical Systems and Signal Processing* 40, 2 (2013) 628–644.
28. G. Xie, D.J. Thompson, C.J.C. Jones: Mode count and modal density of structural systems : Relationships with boundary conditions. *Journal of Sound and Vibration* 274, 3 (2004) 621–651.
29. M. Gérardin, D. Rixen: *Théorie des vibrations. Application à la dynamique des structures*, Ed. Masson, Paris. 1992.
30. E.V. Jansson: Admittance measurements of 25 high quality violins. *Acta Acustica united with Acustica* 83, 2 (1997) 337–341.
31. J.A. Torres, R.R. Boullosa: Influence of the bridge on the vibrations of the top plate of a classical guitar. *Applied Acoustics* 70, 11–12 (2009) 1371–1377.
32. B. Elie, F. Gautier, B. David: Macro parameters describing the mechanical behavior of classical guitars. *Journal of the Acoustical Society of America* 132, 6 (2012) 4013–4024.
33. K. Ege, X. Boutillon: Synthetic description of the piano soundboard mechanical mobility, in *Sydney and Katoomba*, Australia. 2010.
34. E. Skudrzyk: The mean value method of predicting the dynamic response of complex vibrators. *Journal of the Acoustical Society of America* 67, 4 (1980) 1105–1135.
35. M.R. Schroeder: New method of measuring reverberation time. *Journal of the Acoustical Society of America* 66, 2 (1965) 928–944.
36. M.R. Schroeder: Integrated-impulse method measuring sound decay without using impulses. *Journal of the Acoustical Society of America* 66, 2 (1965) 497–500.

**Cite this article as:** Elie B. Cotté B. & Boutillon X. 2022. Physically-based sound synthesis software for Computer-Aided-Design of piano soundboards. *Acta Acustica*, 6, 30.